Optics Communications 410 (2018) 970–976

Contents lists available at ScienceDirect

Optics Communications

journal homepage: www.elsevier.com/locate/optcom

Diode-pumped Alexandrite laser with passive SESAM Q-switching and wavelength tunability

Ufuk Parali [a,b,*], Xin Sheng [a], Ara Minassian [c], Goronwy Tawy [a], Juna Sathian [a], Gabrielle M. Thomas [a], Michael J. Damzen [a]

[a] Photonics Group, The Blackett Laboratory, Imperial College London, London SW7 2AZ, United Kingdom
[b] Department of Electrical and Electronics Engineering, Alanya Alaaddin Keykubat University, Antalya, 07450, Turkey
[c] Unilase Ltd, 1 Filament Walk, Unit G02, London SW18 4GQ, United Kingdom

ARTICLE INFO

Keywords:
Alexandrite
Passively Q-switched lasers
Tunable lasers
Diode-pumped lasers
Birefringent filter plate
SESAM

ABSTRACT

We report the first experimental demonstration of a wavelength tunable passively Q-switched red-diode-end pumped Alexandrite laser using a semiconductor saturable absorber mirror (SESAM). We present the results of the study of passive SESAM Q-switching and wavelength-tuning in continuous diode-pumped Alexandrite lasers in both linear cavity and X-cavity configurations. In the linear cavity configuration, pulsed operation up to 27 kHz repetition rate in fundamental TEM_{00} mode was achieved and maximum average power was 41 mW. The shortest pulse generated was 550 ns (FWHM) and the Q-switched wavelength tuning band spanned was between 740 nm and 755 nm. In the X-cavity configuration, a higher average power up to 73 mW, and obtained with higher pulse energy 6.5 μJ at 11.2 kHz repetition rate, in fundamental TEM_{00} mode with excellent spatial quality $M^2 < 1.1$. The Q-switched wavelength tuning band spanned was between 775 nm and 781 nm.

1. Introduction

Capability of providing different pulse durations (ns/ps/fs) with wavelength tunability in a wide range requires broad emission bandwidth laser sources. Generation of high power ultrashort optical pulses, frequency conversion, optical coherence tomography, nonlinear microscopy and remote sensing applications are some of the examples that these type of laser sources potentially offer as significant benefits [1–4]. Furthermore, for 3-D mapping of (i) spectral indicators of Earth features and high precision ground topography, (ii) atmospheric species and physical attributes, these laser sources provide a powerful tool in air-borne and space-borne remote sensing in laser-based lidar and altimetry such as resonant backscatter lidar and ground vegetation bio-mass/bio-health detection applications [1,5–8]. On the other hand, cutting-edge laser technologies with air-borne and space-borne qualification are needed for these remote sensing applications where strict requirements, especially for space-borne applications, severely narrows the class of lasers that can be utilized in the space environment. Although having narrow linewidth and not allowing wavelength tunability, diode-pumped Nd:YAG laser is one of the main laser systems with long space heritage [1,5]. Providing its higher harmonics at 532 nm and 355 nm, diode-pumped Nd:YAG laser system has only a discrete single frequency as its primary fundamental laser line at 1064 nm. This dictates the utilization of optical parametric conversion methods in these systems for wavelength tunability, causing not only higher complexity and cost but also lower system reliability and efficiency [2–4,9]. Thus, today, the most common alternative approach is the vibronic solid-state laser materials with pulse generation and wavelength tunability capabilities by directly diode laser pumping. Ti:Sapphire, Cr-doped colquiriites (Cr:LiSAF, Cr:LiCAF and Cr:LiSGaF) and Cr-doped chrysoberyl (Cr^{3+}:$BeAl_2O_4$) – more commonly known as Alexandrite – solid-state lasers are the mainly utilized laser systems. However, Ti:Sapphire vibronic laser crystals having the broadest gain bandwidth with the capability of direct generation of a few cycle optical pulses [2,3,10–13] require complex pump sources. This causes tremendous disadvantages such as complex system structure, bulky and large physical size, and low efficiency of electrical–optical conversion [2,12]. Besides, Cr-doped colquiriite lasers are not attractive alternatives, either. Upper-state lifetime quenching at elevated temperatures, poor thermal conductivity and excited state absorption are some of the disadvantages limiting the performance of the Cr-doped colquiriite laser systems [3,10]. On the other hand, among the aforementioned

* Corresponding author at: Department of Electrical and Electronics Engineering, Alanya Alaaddin Keykubat University, Antalya, 07450, Turkey.
E-mail address: ufuk.parali@alanya.edu.tr (U. Parali).

https://doi.org/10.1016/j.optcom.2017.09.047
Received 21 July 2017; Received in revised form 11 September 2017; Accepted 13 September 2017
Available online 4 October 2017
0030-4018/

vibronic solid-state laser gain mediums, due to its number of superior optical and thermo-mechanical properties, Alexandrite is a significantly attractive alternative. Alexandrite has broad absorption bands in the visible range providing the opportunity of direct diode-pumping by red, green and blue laser diodes [3,10]. Providing the highest efficiency and lowest heating factor, however, the red diodes are the most favourable pump sources. The fracture resistance of Alexandrite is five-times bigger than Nd:YAG. Moreover, its thermal conductivity (23 $Wm^{-1}K^{-1}$) [3] is almost twice that of Nd:YAG and five-times that of the Cr-doped colquiriites. Alexandrite crystal eliminates the depolarization problems due to its birefringence. Thus, it has a highly linearly polarized laser emission [2,3]. Due to its unique spectroscopic properties, the laser performance of Alexandrite is increased at elevated temperatures [14]. Moreover, having relatively longer upper-state lifetime (~260 μs) at room temperature, it provides a good energy storage potential for Q-switched operation [2]. Alexandrite has a relatively low stimulated emission cross section (0.7×10^{-20} cm^2) requiring intense diode pumping [3]. Having a broad emission wavelength range from ~700 nm to 850 nm, Alexandrite is the first wavelength tunable solid state laser in the literature operated at room temperature [15–17]. This spectral band, being in the biological window for tissue transmission and sitting across the so-called red-edge band (~700–750 nm) of chlorophyll, is especially important [5]. The red-edge band is the steep rising transition band between high red and visible absorption and high near-IR reflection. Thus, having a laser with emission spectrum covering this red-edge band range is very interesting for a vegetation lidar since changes in this spectral band are well-known as early indicators of plant health [5].

Recently, in our prior work at Imperial College, continuous-wave (cw) red diode-pumped Alexandrite laser with greater than 26 W of average output power was obtained and the first active Q-switching with an electro-optic Pockels cell was achieved [2,18]. Interestingly, the first femtosecond Kerr-lens mode-locked Alexandrite laser was recently reported in [4] producing pulses as short as 170 fs.

In this study, we report the first successful experimental demonstration of a wavelength tunable passively Q-switched Alexandrite laser with semiconductor saturable absorber mirror (SESAM) and using a red diode (AlGaInP) pump laser at 635 nm. We designed two different setups: (1) linear cavity configuration (i) working in TEM_{00} fundamental mode with spatial beam quality $M^2 < 1.7$, (ii) achieving 27 kHz highest repetition rate, (ii) generating 41 mW maximum average output power, (iii) producing 550 ns (FWHM) shortest pulse width and (iv) having wavelength tuning band between 740 nm and 755 nm; (2) X-cavity configuration (i) working in TEM_{00} fundamental mode with spatial beam quality $M^2 < 1.1$, (ii) achieving 11.2 kHz highest repetition rate, (ii) generating 73 mW maximum average output power, (iii) producing 6.9 μs (FWHM) shortest pulse width and (iv) having wavelength tuning band between 775 nm and 782 nm. A birefringent filter (BiFi) plate was used in both of the cavities for tuning the wavelength of the laser. To the best of our knowledge, this is the first wavelength tunable TEM_{00} passive Q-switching operation of a red diode-pumped Alexandrite laser. Our results open the way for further development, optimization and power scaling of this new generation passively Q-switched Alexandrite lasers. One interesting application for developing a compact, low-cost and wavelength tunable pulsed laser source is space-borne and air-borne remote sensing applications, especially for the next generation vegetation lidar systems. We acknowledge the Photoptics 2017 conference where some part and results of this study has been presented [19].

2. Linear cavity experimental laser system

We designed a simple linear cavity for studying the wavelength tunable passive Q-switching operation mode of the direct diode-pumped Alexandrite laser. Two experimental systems are described for this purpose. As a precursor study, Fig. 1 shows the first system for a wavelength tunable cw setup. Fig. 2 shows the second system for a wavelength tunable passively Q-switched laser setup using a semiconductor saturable absorber mirror.

The wavelength tunable cw laser had a plane–plane mirror cavity. The Alexandrite rod crystal gain medium was doped with 0.22% of Cr^{3+} and *c*-axis cut with 10 mm length and 4 mm diameter. The end faces of the rod were plane-parallel and anti-reflection coated at the Alexandrite wavelength (~755 nm). The rod crystal was mounted in water-cooled copper heat-sink where an indium foil interface was used for enhancing the thermal contact to the copper. The cavity length was ~142 mm. An intracavity plano-convex lens (PCX, $f = 70$ mm) was located in the cavity where the intracavity lens design was chosen not only to form a stable cavity configuration but also to optimize for TEM_{00} operation. A dichroic back mirror (BM) with highly-reflecting (R > 99.9%) at laser wavelength (~755 nm) and highly-transmitting (R < 0.2%) for pump diode laser (~635 nm) was utilized. We used a single water chiller in the experiments for cooling both the temperature of the Alexandrite crystal and the pump laser diode to 16 °C.

The small-signal absorption coefficient (α) of the crystal was measured as ~6 cm^{-1} with a He–Ne laser at 633 nm for light polarized parallel to the *b*-axis of Alexandrite crystal. A red diode module operating nominally at central wavelength 635 nm was utilized for pumping the crystal. The bandwidth (FWHM) of the pump module was ~1.5 nm and capable of providing max ~5 W (5180 mW full power) in cw mode. It was fibre coupled in a multi-mode fibre with core diameter of 105 μm and numerical aperture of 0.22. The pump beam output from the fibre was collimated utilizing an aspheric fibre collimator with 35 mm of focal length. The circularized pump beam was focused into a ~120 μm spot size diameter inside the crystal by an aspheric pump lens (ASP) of 50 mm focal length.

The output of the fibre was not a pure polarization where >60% was in the highly absorbing *b*-axis direction of the Alexandrite crystal absorbing about 83% of the pump power. The absorption depth of the crystal allowing good laser mode overlap with the pump was shorter than the confocal parameter of the *b*-axis component of the pump (~4 mm). The overlap of the laser mode to the other polarization however would be poor which will diminish the efficiency of the system.

A quartz plate with a thickness of 0.5 mm acting as a birefringent filter (BiFi) tuner is utilized for tuning the wavelength of the laser. In order to minimize the insertion losses, the BiFi is placed in the cavity at Brewster angle. The wavelength is tuned rotating the BiFi in the plane of the plate with a goniometer to alter the birefringence of the plate and spectral window for lasing. This provided simplicity for both of the cavities (Figs. 1 and 2) working in cw and passive Q-switching mode in tuning the wavelength of the laser output.

For optimizing the laser cavity and as a reference, we first obtained the cw mode of operation by using an output coupler (OC) with 99.5% reflectivity (Fig. 1). To obtain passive Q-switching mode (Fig. 2), we replaced the OC with a SESAM as the end mirror with the output beam obtained from leakage from the BiFi. The SESAM was attached on an aluminium disc using thermal adhesive for helping to increase the heat transfer between SESAM and the aluminium. We used the SESAM as the end mirror in the cavity. The beam spot size diameter on the SESAM was calculated to be ~250 μm. SESAM samples used were based on multiple layers of InP quantum dots on a distributed Bragg reflector [20,21]. They had a saturable absorption with modulation depth ~ 0.5% and had also some non-saturable loss (~1%) where both the non-saturable loss and modulation depth were wavelength dependent. The SESAM mirror structure had a ~60 nm reflectivity bandwidth centred at ~740 nm (R ~ 99%) and a ~10 nm (FWHM) photoluminescence band positioned near the reflectivity centre. The dynamic response (absorption recovery) of the SESAM was bi-exponential with <0.5 ps for fast component and ~300 ps for slow component. The saturation fluence was ~30 $\mu J/cm^2$.

3. Results of the CW and passively Q-switched Alexandrite laser

Firstly, the variation of the CW output power as a function of emission wavelength was investigated in our initial experiments as shown in Fig. 3, using the 99.5% reflectivity output coupler at maximum

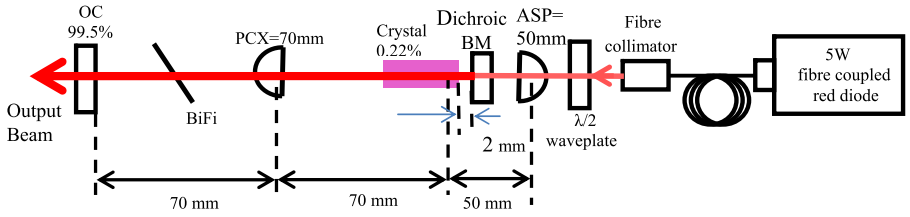

Fig. 1. Schematic layout of the plane–plane mirror cavity wavelength tunable continuous-wave direct red diode-pumped Alexandrite laser operating in fundamental TEM_{00} mode.

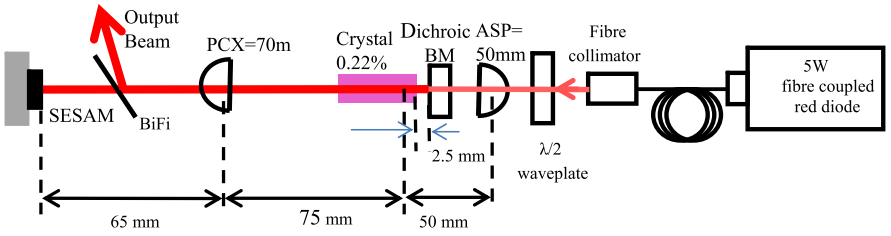

Fig. 2. Schematic layout of the wavelength tunable passively Q-switched direct red diode-pumped Alexandrite laser. Here, OC in Fig. 1 is replaced with SESAM. The output coupling is provided from the reflection of the BiFi in the cavity.

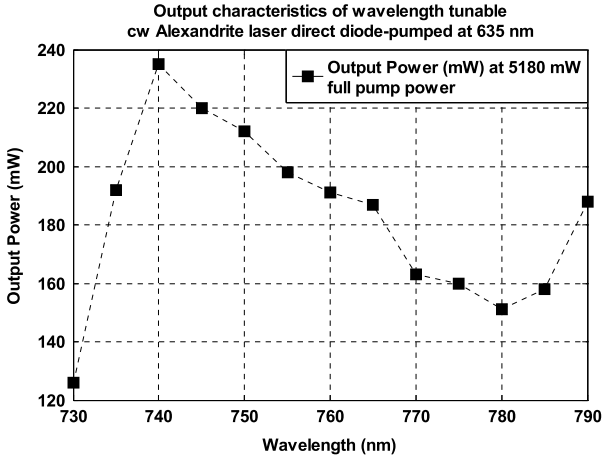

Fig. 3. Tuning curve for the cw Alexandrite laser with 0.5 mm BiFi tuner plate. Alexandrite crystal temperature was 16 °C, output coupler was 0.5% transmitting, and incident pump power was 5180 mW.

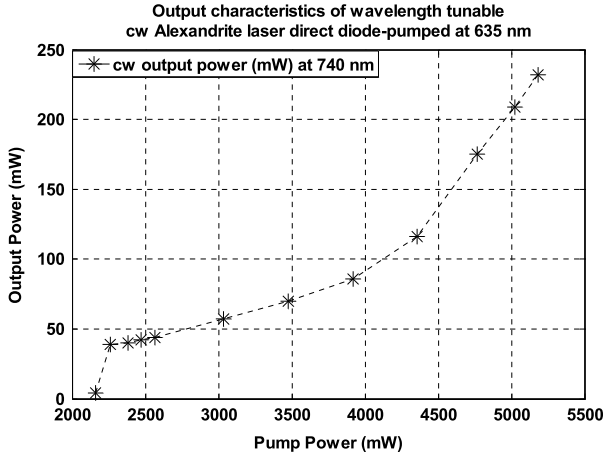

Fig. 4. Output power vs Pump power curve of cw Alexandrite laser cavity at constant wavelength of $\lambda = 740$ nm. Laser crystal is at 16 °C and 0.5% transmitting output coupler.

pumping power 5180 mW. Tuning in the range extended from 730 nm to 790 nm was obtained. Typical lasing spectral bandwidth was ~0.5 nm but may have been limited by the spectral resolution of our spectrometer (~0.5 nm). Although a much wider tuning range was possible as can be seen from Fig. 3, the main focus of this study was operation around the wavelength band of the SESAM device.

Fig. 4 shows the measured CW output power versus the pump power curve of the cavity for fixed laser output wavelength at 740 nm. The slope efficiency was ~14% at the highest output power, and it shows no sign of decrement, suggesting that the output power is not limited by the thermal lensing effects. As can be further seen in Fig. 4, with the available pump power, the slope efficiency and output power keeps increasing. This suggests that utilizing more powerful pump lasers, it is possible to further improve the power performance of the laser. The optical-to-optical efficiency with respect to incident pump power can also be expected to be considerably increased by optimizing output coupling, reducing intracavity loss and attention to spectral profile of coated cavity optics.

We replaced the OC mirror with the SESAM for passive Q-switching the Alexandrite laser once the characterization of the wavelength tunable cw laser cavity was completed. The output of the laser was provided by a reflection loss from the BiFi plate. Fig. 2 shows the dimensions of the Alexandrite laser working in a self-Q-switched mode. Due to the spot size on the SESAM, the position of the intracavity lens in the cavity particularly showed a strong effect on the output power after the alignment of the cavity was optimized.

Fig. 5 shows the evolution of the output power, pulse width and the repetition rate with respect to the pump power at constant wavelength $\lambda = 747$ nm by fixing the BiFi at appropriate angle. Due to the larger losses incurred by the insertion of the SESAM, it is noted that the cavity has a higher threshold. Shorter pulses with higher repetition rate were obtained as the available pump power increases above threshold.

Intracavity losses limited the slope efficiency which can be improved by careful loss management. Besides, the output beam is obtained from the BiFi in the cavity. Although this is not the best configuration for obtaining the output pulse from a laser cavity, our objective in choosing this setup was to make the system as simple as possible in order to just show experimentally for the first time that the diode-pumped Alexandrite crystal can be passively Q-switched.

The evolution of the output power, pulse width, repetition rate and spectral width of the pulses obtained from the passively Q-switched diode-pumped Alexandrite laser in the wavelength tunability range for full pump power is depicted in Fig. 6. For tuning the passively Q-switched Alexandrite laser, we again used the BiFi inside the cavity.

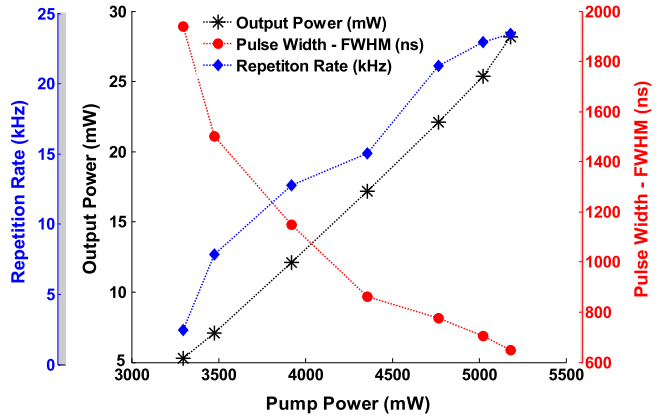

Fig. 5. For constant wavelength λ = 747 nm, the evolution of the output power, pulse width and the repetition rate of the passively Q-switched diode-pumped Alexandrite laser with respect to the 635 nm pump power.

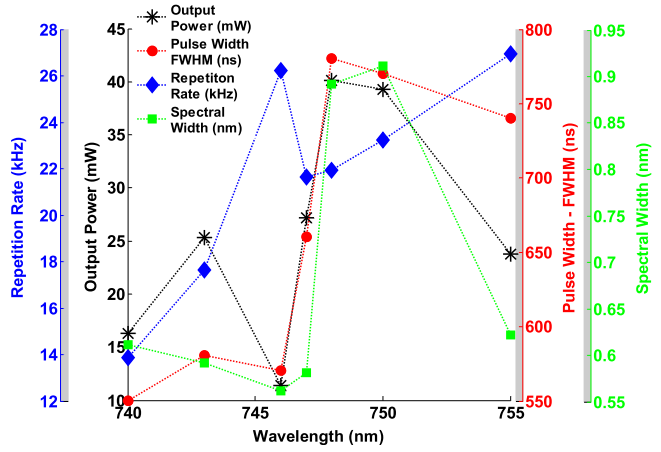

Fig. 6. The output power, pulse width, repetition rate and spectral width of the pulses obtained in the wavelength tunability range from the passively Q-switched Alexandrite laser.

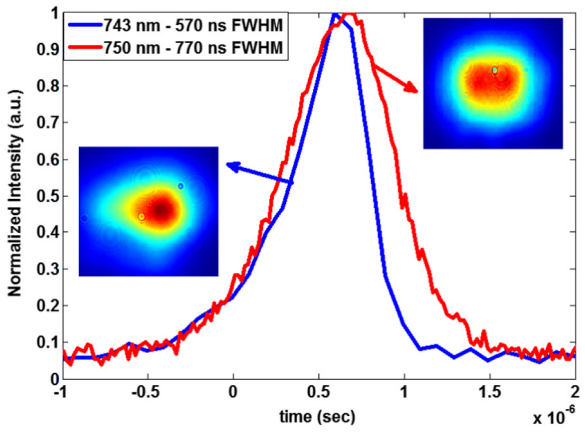

Fig. 7. Pulse profiles and spatial profiles obtained at 743 nm and 750 nm from the tunable passively Q-switched Alexandrite laser.

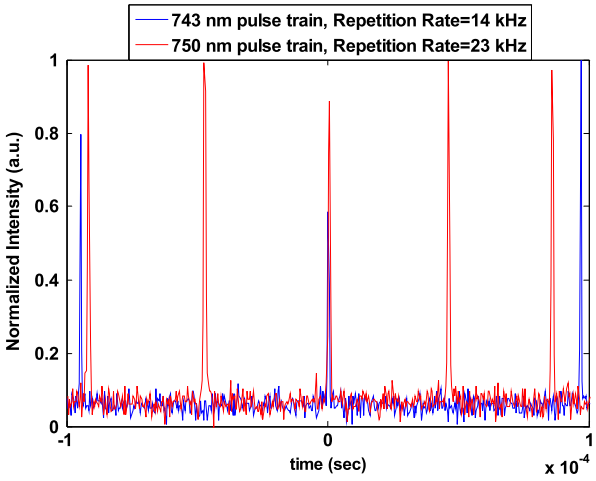

Fig. 8. Pulse train observed from passively Q-switched Alexandrite laser at 743 nm and 750 nm with repetition rates of 14 kHz and 23 kHz, respectively.

In this instance, the tunability of the system was restricted by (i) the limited reflectivity band of the SESAM and (ii) the range over which Q-switching could be accomplished. Thus, the achieved tuning bandwidth was between 740 nm and 755 nm shown in Fig. 6 where the Q-switching tuning bandwidth is narrower than the CW tuning range shown in Fig. 3.

The highest pulse repetition rate was 27 kHz at 755 nm and the shortest pulse width was 550 ns at 740 nm. The observed spectral width was <1 nm throughout the tuning range of the passive Q-switching mode. Maximum output power was 41 mW at repetition rate 22 kHz (corresponding to pulse energy ~ 2 μJ). Taking the mode diameter size on the SESAM as ~250 μm and the intracavity round-trip loss as 5%, the estimated intracavity fluence on the SESAM was ~ 0.2 J/cm^2, so the saturable absorption component of SESAM device can be expected to be fully saturated (E_{sat} ~ 30 μJ/cm^2).

The pulse widths and the spatial profiles obtained at the wavelengths of 743 nm and 750 nm using full pump power are compared in Fig. 7. The laser output beams for both wavelengths had TEM_{00} beam profile with M^2 values <1.7 and <1.9 for 743 nm and 750 nm, respectively. The M^2 beam quality was determined using the ISO 11146-1 method, based on the second moment beam size. Due to the increased mode-gain overlap in the cavity, higher output power was achieved when the mode of the beam profile was adjusted to higher spatial modes.

The pulse train and the repetition rates obtained at the wavelengths of 743 nm and 750 nm using full pump power are depicted in Fig. 8. Pulse repetition rates of 14 kHz and 23 kHz are obtained at the wavelength of 743 nm and 750 nm, respectively. Here, the stability of passive Q-switching operation mode of linear cavity setup is relatively low comparing to the stability of X-cavity setup as described in Section 4 of this paper.

4. X-cavity experimental laser system

We note that in order to demonstrate the wavelength tunable passively Q-switched direct diode-pumped Alexandrite laser experimentally for the first time, we choice to utilize a very simple linear cavity configuration. However the configuration has some disadvantages especially in terms of efficiency, in particular, the use of the output coupling of the beam coming from the BiFi was not ideal. In order to overcome this issue, we developed an X-cavity setup as explained below.

Fig. 9 shows the wavelength tunable passively Q-switched X-cavity diode-pumped Alexandrite laser. The gain medium was a Brewster angle cut Alexandrite rod with a length of 8 mm and a diameter of 4 mm doped with 0.22% of Cr^{3+}. The Alexandrite rod was mounted in a water-cooled copper heat-sink with its *b*-axis orientated horizontally. A pair of curved mirrors (CM1 and CM2) with radii of curvature of $R = -100$ mm is used to form the X-cavity with an output coupler mirror in one arm and a back mirror in the other arm, either the SESAM or, in initial measurements, a plane high reflectivity mirror. The 0.5 mm thick birefringent tuning plate was inserted in the output coupler arm for wavelength tuning. The

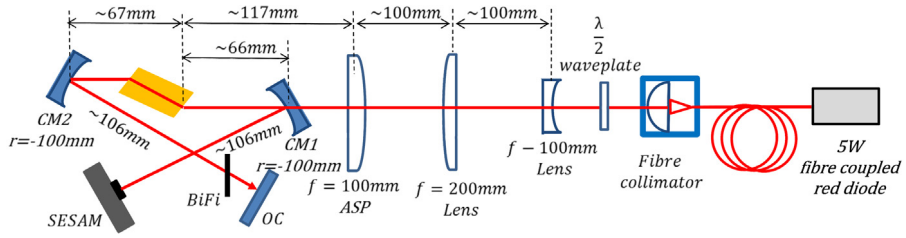

Fig. 9. Schematic of wavelength tunable passively Q-switched X-cavity diode-pumped Alexandrite laser.

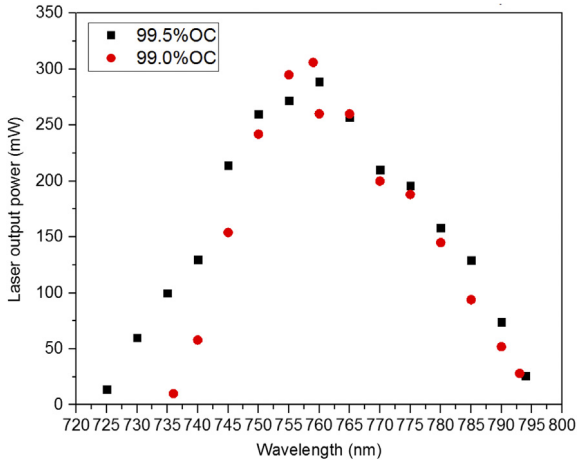

Fig. 10. Tuning curves for X-shaped CW Alexandrite laser (output couplers R = 99.0% and R = 99.5%).

SESAM in this system was a second sample with similar characteristics to the previous one except a reflectivity band ~60 nm centred on ~760 nm.

A similar fibre delivered red diode module described in the previous section was utilized, operating nominally at central wavelength 635 nm with bandwidth (FWHM) of 1.5 nm. Because of the limited space caused by the curved pump through mirror, the pump f = 50 mm aspheric focusing lens was replaced by a f = 100 mm aspheric lens preceded by a two-element telescope system (f = −100 mm and f = 200 mm), the whole system should give the identical pump beam waist size on the front face of the crystal as the f = 50 mm aspheric lens. In reality, this was not the case. The presence of the angled plano-concave cavity mirror (CM1) acts as an astigmatic negative lens that increases the pump size and negatively impacts the pump beam M^2 quality.

The output power of the X-shaped Alexandrite laser for an R = 99.0% output coupler and plane HR back mirror with no birefringent tuner was 460 mW. The wavelength tunability of the X-shaped Alexandrite laser cavity with BiFi tuner is shown in Fig. 10 for two different output couplers (reflectivity 99% and 99.5%). With the 99.0% reflectivity output coupler tuning was from 736 nm to 793 nm and maximum output power of 306 mW was obtained at 759 nm. For the R = 99.5% output coupler, the laser wavelength was tuned in the range extended from 725 nm to 794 nm. Maximum output power of 290 mW was obtained. The short wavelength cut-off was found to correlate to a sharp fall in mirror reflectivity near 730–740 nm for the 99% coupler and a sharp fall in reflectivity near 720–730 nm for the 99.5% coupler.

For the SESAM passively Q-switched system, Fig. 11a shows the output pulse train which were obtained with R = 99.0% OC at ~778 nm, and with the spectral width (FWHM) of 0.32 nm. The average power of 73 mW and the repetition rates of 11.2 kHz resulted in the Q-switched pulse energy of 6.5 μJ with pulse width of 6.9 μs. The relatively large pulse duration is due to the long cavity photon lifetime due to the large cavity length (345 mm) and the highly reflective output coupler we used (R = 99.0%). Here, the stability of passive Q-switching operation mode of the X-cavity setup is relatively very high comparing to the stability (see Fig. 8) of linear cavity setup. The beam from the output coupler was imaged by a relay-imaging system onto a CMOS camera (Fig. 11b). The laser beam waist has a diameter of ~288 μm (x) by ~326 μm (y) with M^2 < 1.1 in both axes. Because of the symmetry of the laser cavity system, the beam size on the SESAM is roughly the same as the beam size on the OC.

Fig. 12 shows the results of the output power of the passively SESAM Q-switched Alexandrite laser against incident pump power for the two output couplers with reflectivity R = 99.0% and R = 99.5%. For these power curves the BiFi was temporally taken out of the cavity to remove its insertion loss. The threshold for the 99% coupler was higher than the 99.5% coupler but had higher slope efficiency. For the 99.5% output coupler a shortest pulse duration of 3.4 μs was obtained at 16.7 kHz for 4.2W pump power and 76 mW output power (4.6 μJ pulse energy). For the 99% output coupler shortest pulse was 5.3 μs at 10.7 kHz and 90 mW output power (8.4 μJ pulse energy) at 4.8 W pumping.

For investigating the wavelength tunability of the system the BiFi was inserted. The average output power, pulse width, and repetition rate obtained across the wavelength tuning range for the passively Q-switched Alexandrite laser are summarized in Fig. 13.

The maximum average output power 73 mW was obtained at 778 nm at 11.2 kHz pulse rate (corresponding to 6.5 μJ pulse energy). Tuning range for passive Q-switching was between 775–781 nm. It is noted the X-cavity gave higher efficiency overall than the linear cavity. However, with further improvements in pumping beam quality and cavity design much higher efficiency is expected from this cavity configuration.

5. Conclusion

We have reported the first demonstration of passively SESAM Q-switched with BiFi wavelength-tuned operating in fundamental TEM_{00} mode Alexandrite laser under continuous-wave diode-pumping. In our experiments, we developed two different laser cavity configurations. In the first Q-switched system with linear cavity design, the wavelength tuning band spanned between 740 nm and 755 nm, the highest repetition rate achieved was 27 kHz and the maximum average output power obtained was 41 mW, and the shortest pulse generated was 550 ns (FWHM). The spatial quality was M^2 < 1.7. In the second Q-switched system with X-cavity design, the wavelength tuning band spanned between 775 nm and 781 nm, with maximum repetition rate 11.2 kHz at 778 nm and average output power 73 mW, corresponding to 6.5 μJ pulse energy. The beam was TEM_{00} mode with excellent spatial quality M^2 < 1.1 in both axes measured.

It is noted that this work was not fully optimized for efficiency. Thus, the results obtained in this study pave the way for further development, optimization and power scaling of this new generation direct diode-pumped wavelength tunable passively Q-switched (and also potentially for passively mode-locked) Alexandrite laser. No intra-cavity optical damage occurred in both of the cavity configurations during passive Q-switching. Thus, further pump optimization is expected to increase average output power and efficiency and reduce pulse duration. Improved pump sources would enable both higher power

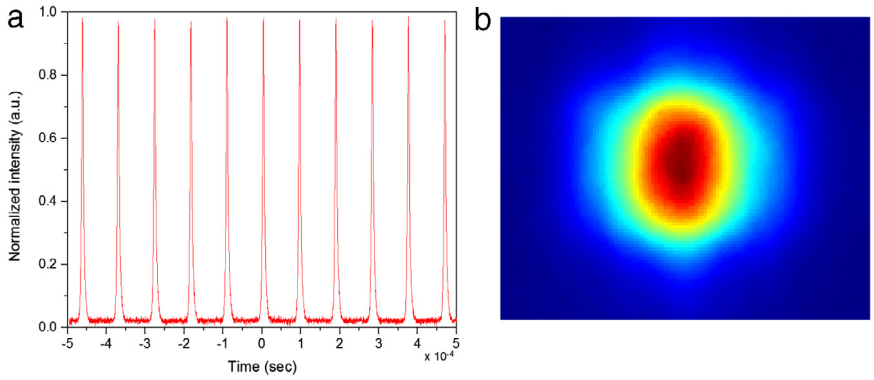

Fig. 11. (a) Pulse train observed from passively Q-switched Alexandrite laser with $R = 99.0\%$ OC at ~778 nm (pulse repetition rates of 11.2 kHz) and, (b) spatial profile of output beam.

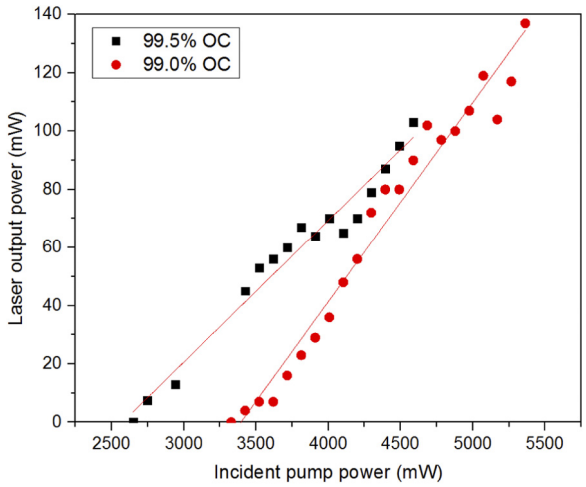

Fig. 12. Laser output power against incident pump power for passively Q-switched X-cavity Alexandrite laser for $R = 99.5\%$ and $R = 99.0\%$ output coupler.

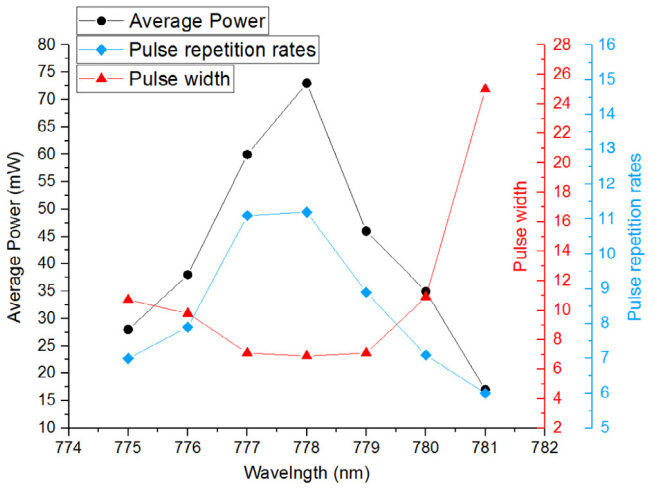

Fig. 13. Average output power (mW), pulse width (μs) and repetition rate (kHz) obtained within wavelength tuning range for the passively Q-switched X-cavity Alexandrite laser.

scaling and higher efficiency. Furthermore, higher crystal temperature, higher doping concentration, longer gain medium, optimized (reduced) output coupler reflectivity, and careful intracavity loss management (such as pump excited state absorption) will provide us to obtain better performance and efficiency enhancement in the tunable Q-switched operation of diode-pumped Alexandrite laser.

Due to the promising results shown and the superior optical and thermo-mechanical properties comparing with its counterparts, this new generation direct diode-pumped, wavelength tunable, compact, low-cost and efficient passively Q-switched Alexandrite laser has interesting potential for future applications.

Acknowledgements

We would like to acknowledge support from the British Council and Newton Fund under Project No. 215277462. U.P. would like to acknowledge support from TÜBİTAK 1059B191401929 (The Scientific and Technological Research Council of Turkey) for his visit to Imperial College London. The authors acknowledge J.E. Hastie, V.G. Savitski and M.D. Dawson from the Institute of Photonics, University of Strathclyde, Glasgow who developed and characterized the SESAM samples used in this study and A. Krysa from the National Centre for III–V Technologies, University of Sheffield who grew them under EPSRC project EP/E056989/1. We would also like to thank Dr A. Major from the University of Manitoba for kindly sharing these SESAM samples to enable us to perform this study.

References

[1] M.J. Damzen, G.M. Thomas, A. Teppitaksak, A. Minassian, Progress in diode-pumped Alexandrite lasers as a new resource for future space lidar missions, in: ICSO International Conference on Space Optics, 2014.
[2] A. Teppitaksak, A. Minassian, G.M. Thomas, M.J. Damzen, High efficiency >26 w diode end-pumped Alexandrite laser, Opt. Express 22 (2014) 16386–16392.
[3] W. Koechner, M. Bass, Solid-State Lasers: Graduate Text, Springer-Verlag, New York, 2003.
[4] S. Ghanbari, R. Akbari, A. Major, Femtosecond Kerr-lens mode-locked Alexandrite laser, Opt. Express 24 (2016) 14836.
[5] J.U.H. Eitel, L.A. Vierling, M.E. Litvak, D.S. Long, Broadband, red-edge information from satellites improves early stress detection in a New Mexico conifer woodland, Remote Sens. Environ. 115 (2011) 3636–3640.
[6] T. Lu, H. Li, Atmospheric turbulence induced synthetic aperture lidar phase error compensation, Opt. Commun. 381 (2016) 214–221.
[7] J. Pelon, G. Megie, C. Loth, P. Flamant, Narrow bandwidth Q-switch alexandrite laser for atmospheric applications, 59(3) (1986) 213-218.
[8] M.J.T. Milton, T.D. Gardiner, F. Molero, J. Galech, Injection seeded optical parametric oscillator for range-resolved DIAL measurements of atmospheric methane, Opt. Commun. 142 (1997) 153–160.
[9] A. Teppitaksak, G.M. Thomas, M.J. Damzen, Investigation of a versatile pulsed laser source based on a diode seed and ultra-high gain bounce geometry amplifiers, Opt. Express 23 (2015) 12328–12336.
[10] S. Ghanbari, A. Major, High power continuous-wave Alexandrite laser with green pump, Laser Phys. 26 (2016) 075001.
[11] E. Beyatli, I. Baali, B. Sumpf, G. Erbert, A. Leitenstorfer, A. Sennaroglu, U. Demirbas, Tapered diode- pumped continuous-wave alexandrite laser, J. Opt. Soc. Amer. B 30 (2013) 3184–3192.
[12] U. Demirbas, D. Li, J.R. Birge, A. Sennaroglu, G.S. Petrich, A. Kolodziejski, F.X. Kartner, J.G. Fujimoto, Low-cost, single-mode diode-pumped Cr:Colquiriite lasers, Opt. Express 17 (2009).

[13] A. Sennaroglu, F.X. Kaertner, J.G. Fujimoto, Low-threshold, room-temperature femtosecond cr^{4+}:forsterite Laser, Opt. Express 15 (2007).
[14] P. Loiko, A. Major, Dispersive properties of Alexandrite and beryllium hexaaluminate crystals, Opt. Express 6 (2016).
[15] W.R. Kerridge-Johns, M.J. Damzen, Analytical model of tunable Alexandrite lasing under diode end-pumping with experimental comparison, J. Opt. Soc. Amer. B 33 (2016) 125002.
[16] J.C. Walling, D.F. Heller, H. Samelson, D.J. Harter, J.A. Pete, R.C. Morris, Tunable Alexandrite lasers: Development and performance, J. Quantum Electronics QE 21 (1985) 1568–1581.
[17] C.L. Sam, J.C. Walling, H.P. Jenssen, R.C. Morris, E.W. O'Dell, Characteristics of alexandrite lasers in Q-switched and tuned operations, Adv. Laser Eng. Appl. 247 (1980) 130–136.
[18] G.M. Thomas, A. Minassian, X. Sheng, M.J. Damzen, Diode-pumped Alexandrite lasers in Q-switched and cavity- dumped Q-switched operation, Opt. Express 24 (2016) 27212–27224.
[19] U. Parali, G.M. Thomas, A. Minassian, X. Sheng, M.J. Damzen, Wavelength tunable passively Q-switched Alexandrite laser with direct diode-pumping at 635 nm, in :Proceedings of the 5th International Conference on Photonics, Optics and Laser Technology - Volume 1: Photoptics, ISBN: 978-989-758-223-3, 2017, pp. 82–89.
[20] P.J. Schlosser, J.E. Hastie, S. Calvez, A. Krysa, M.D. Dawson, InP/AlGaInP quantum dot semiconductor disk lasers for CW TEM00 emission at 716-755 nm, Opt. Express 17 (2009) 21782–21787.
[21] V.G. Savitski, P.J. Schlosser, J.E. Hastie, A. Krysa, M.D. Dawson, D. Burns, S. Calvez, Passive mode-locking of a Ti: Sapphire laserby ingap quantum-dot saturable absorber, IEEE Photonics Technol. Lett. 22 (2010) 209–211.